Electronic Supplementary Material (ESI) for Nanoscale.
This journal is © The Royal Society of Chemistry 2016

Electronic Supplementary Information (ESI) for

Pure white-light emitting ultrasmall organic-inorganic hybrid perovskite nanoclusters

Meghan B. Teunis,[‡] Katie N. Lawrence,[‡] Poulami Dutta,[§] Amanda P. Siegel,[‡] and Rajesh Sardar[‡,*]

[‡]Department of Chemistry and Chemical Biology, Indiana University-Purdue University Indianapolis, 402 N. Blackford Street, Indianapolis, Indiana 46202, United States

[§]Department of Chemistry, Michigan State University, 578 South Shaw Lane, East Lansing, Michigan 48824, United States

*Email: rsardar@iupui.edu

Chemicals: Lead (II) bromide ($PbBr_2$, 99.999%), methylamine solution (CH_3NH_2 2.0 M in THF), hydrobromic acid (HBr, 48%), 1-octadecene (ODE, 90%), hexylamine (HA 99%), 1,12-diaminododecane (DADD, 99%), acetone (99.5%, ACS reagent), N,N-dimethylformamide (DMF) were purchased from Sigma-Aldrich. Hydrochloric acid (HCl, 37%) was purchased from Fisher Scientific. ODE was kept under high vacuum overnight and transferred to the glovebox under N_2 atmosphere prior to use. Polyurethane beads were purchased from Fluka. All solvents were purged with N_2 for 30 min prior to use. Bulk methylammonium lead bromide ($MAPbBr_3$) single crystals were grown according to the literature procedure[1] for X-ray diffraction analysis.

Synthesis of methylammonium bromide (CH_3NH_3Br): CH_3NH_3Br was synthesized according to the literature procedure.[2] Briefly, an equivalent amount of HBr was added drop-wise to a solution of methylamine in ethanol (20 mL) at 0°C. The reaction mixture was stirred for 3 hr and then solvent was removed by rotary evaporation and the solid was dissolved in a minimum amount of ethanol and recrystallized by adding ether. The solid was then dried under vacuum producing a snow-white crystalline material that was inside a N_2 filled glove box for further use. CH_3NH_3Br was synthesized under identical mole ratio of the reagents and similar experimental procedure.

Spectroscopy and microscopy characterization

UV-vis absorbance. Absorption spectra were collected with a Varian Cary 50 Scan UV-visible spectrophotometer using a 1 cm quartz cuvette over the range of 300-800 nm. All spectra were collected in toluene, which was used as a background for these measurements.

Ground state photoluminescence, excited state lifetime, and absolute quantum yield measurements. The photoluminescence (PL) emission spectra were acquired using a Cary Eclipse fluorescence spectrophotometer from Varian Instruments using a 1 cm quartz cuvette. The lifetime measurements were recorded using a time-correlated single photon counting (TCSPC) experimental set up. The data acquisition card (DAQ) was from Edinburgh Instrument (TCC900). The laser was a 405 nm pulsed laser from PICOQUANT (LDH-D-C-405M. CW-80MHz) with pulse width < 100 ps. The detector was a photomultiplier tube (PMT) from the HAMAMATSU (HT422-40). The following stretched-exponential equation was used to determine the excited state lifetime.[3]

$$\langle t \rangle = \tau_{av} = \frac{\int_0^{\infty} g(t)t\,dt}{\int_0^{\infty} g(t)\,dt} = \frac{1}{\Gamma_{str}\beta}\bar{\Gamma}\left(\frac{1}{\beta}\right),$$

^{1}H NMR characterization. The ^{1}H NMR spectra were obtained with a Bruker AVANCE III 500 instrument at 500 mHz frequency. Typically, ~10-15 mg of purified sample was dissolved on 0.6 mL of chloroform-d at room temperature. Minimum of 1024 scans were collected with a 30° pulse angle, 3 sec acquisition, and 3 sec of relaxation. All data were plotted via TOPSPIN 2.1 software.

Transmission electron microscopy (TEM) characterization. For TEM analysis, samples were prepared inside a glove box by placing 10 µL of dissolved perovskite nanoclusters (PNCs) in toluene onto a carbon-coated copper grid (Electron Microscopy Science). The sample was allowed to sit for 30 seconds and any excess solution was removed by wicking with a Kimwipe to avoid aggregation. Images were obtained using a JEOL-3200FS-JEM instrument at 200 kV beam energy. The size of the PNCs was determined using ImageJ software.

Energy dispersive X-ray (EDX) analysis. EDX analysis was performed using a Hitachi S-4700 field emission scanning electron microscope. The measurements were conducted at a pressure of $<5 \times 10^{-9}$ Torr. For EDX analysis, the PNCs were drop-casted on a piranha-cleaned silicon wafer inside a N_2 filled glove box, and the solution was allowed to evaporate at room temperature. (*Warning*: piranha solution is highly reactive and must be handled with extreme caution. It reacts violently with organic materials and may not be stored in tightly closed vessels). Before use, piranha-cleaned wafers were washed with copious amounts of Nanopure water and ethanol, and then dried in a vacuum oven at 120° C overnight.

Powder X-ray diffraction (XRD) analysis. XRD analysis was conducted using a Bruker D8 Discover X-Ray Diffractometer. An IµS microfocus X-ray source was used, and the operating voltage and current were 50 kV and 1000 mA, respectively. A thin film of PNCs was prepared on a piranha cleaned glass coverslip by drop-casting the toluene solution of dissolved PNCs inside the glove box. By using Scherrer equation [full width half maximum and angle of (002)] we determined the mean diameter of our $MAPbBr_3$ PNCs.

Synthesis and purification of white-light emitting $MAPbBr_3$ PNCs. Under optimized reaction condition, 2 mL of ODE was placed in a 25 mL 1-neck round bottom flask and stirred at 90° C for 45 min and then 0.067 mmol DADD and 0.03mmol HA were added simultaneously and stirred for an additional 30 min. Separately, 0.032 mmol of CH_3NH_3Br and 0.1 mmol of $PbBr_2$ were dissolved in 100 µL and 200 µL of DMF, respectively. The CH_3NH_3Br was added to the round bottom flask first and allowed to react for 30 sec and then the $PbBr_2$ solution was added. The reaction was allowed to run for 3 min and then the entire solution was quenched by adding 10 mL of acetone resulting in the formation of a white solid. The solid was centrifuged at 5000 rpm for 5 minutes, dissolved in toluene and centrifuged at 7000 rpm for 2 min. The colorless supernatant was collected and dried using a rotavap before being stored in the glove box for further characterization.

Chloride substitution. In a typical substitution, ~4 mg of the purified $MAPbBr_3$ PNCs were dissolved in 5 mL of toluene and allowed to stir for 15 min at room temperature inside the glove box. Then, 0.05 mmol of solid CH_3NH_3Cl was added and the solution was stirred for 1 hr. The insoluble materials (CH_3NH_3Cl and CH3NH3Br are insoluble in toluene) were removed via centrifugation at 5000 RPM for 2 minutes and the solution was collected. White solid was obtained by drop wise additional of acetone. The solid then collected via centrifugation and dried under N_2 flow.

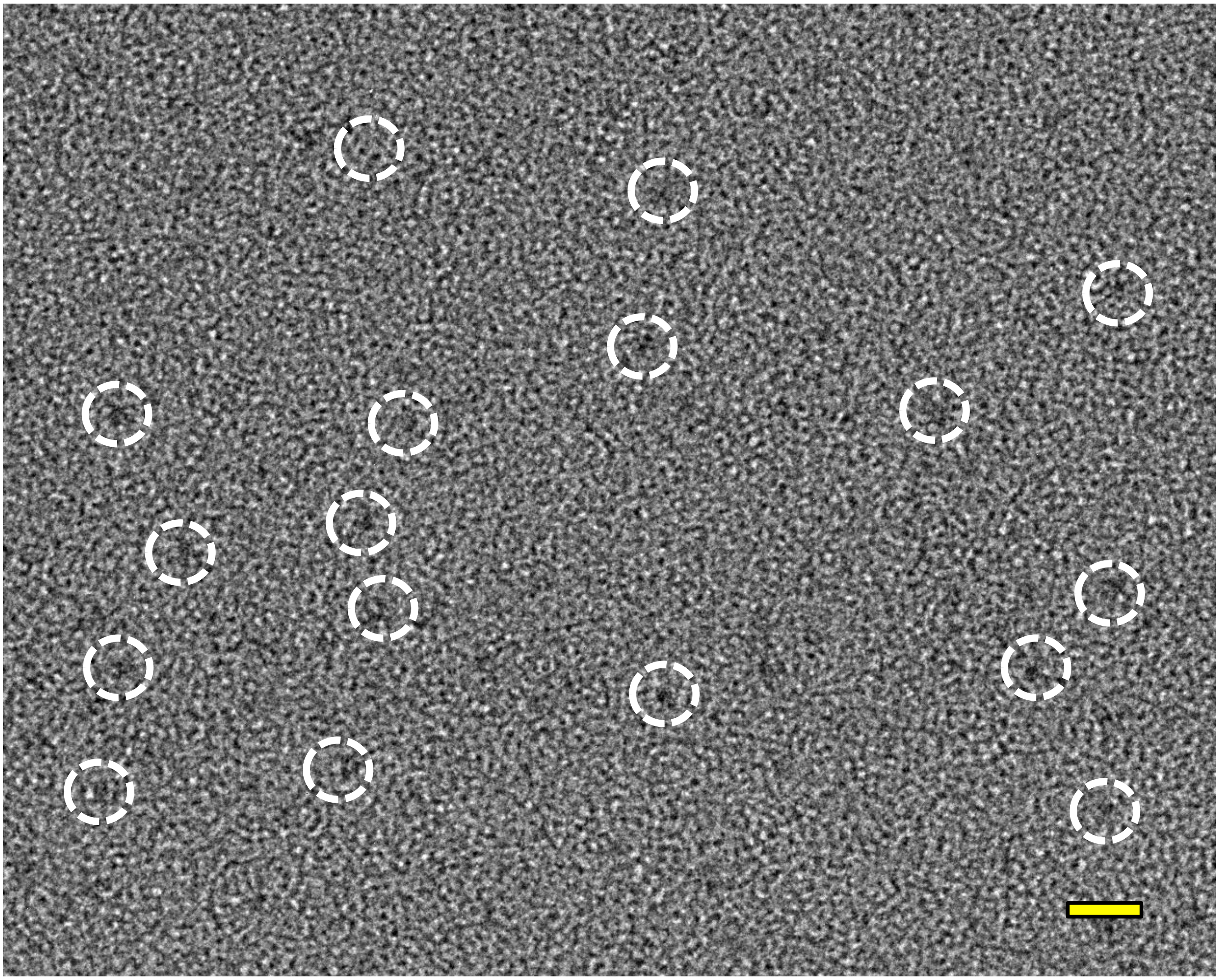

Fig. S1: Structural characterization of MAPbBr$_{3.8}$ PNCs. High-resolution TEM image of ultrasmall MAPbBr$_{3.8}$ PNCs. Dotted white circles represent individual PNC. The scale bar is 10 nm.

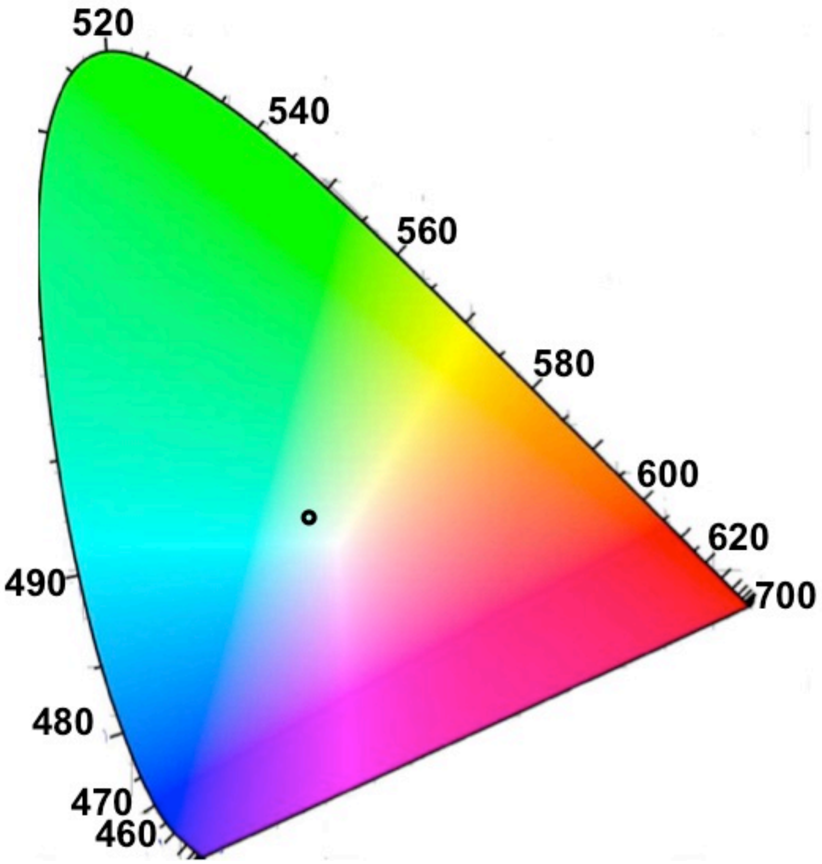

Fig. S2: CIE coordinates of $MAPbBr_{3.8}$ PNCs. The CIE coordinates of ultrasmall $MAPbBr_{3.8}$ PNCs were found to be (0.304, 0.351).

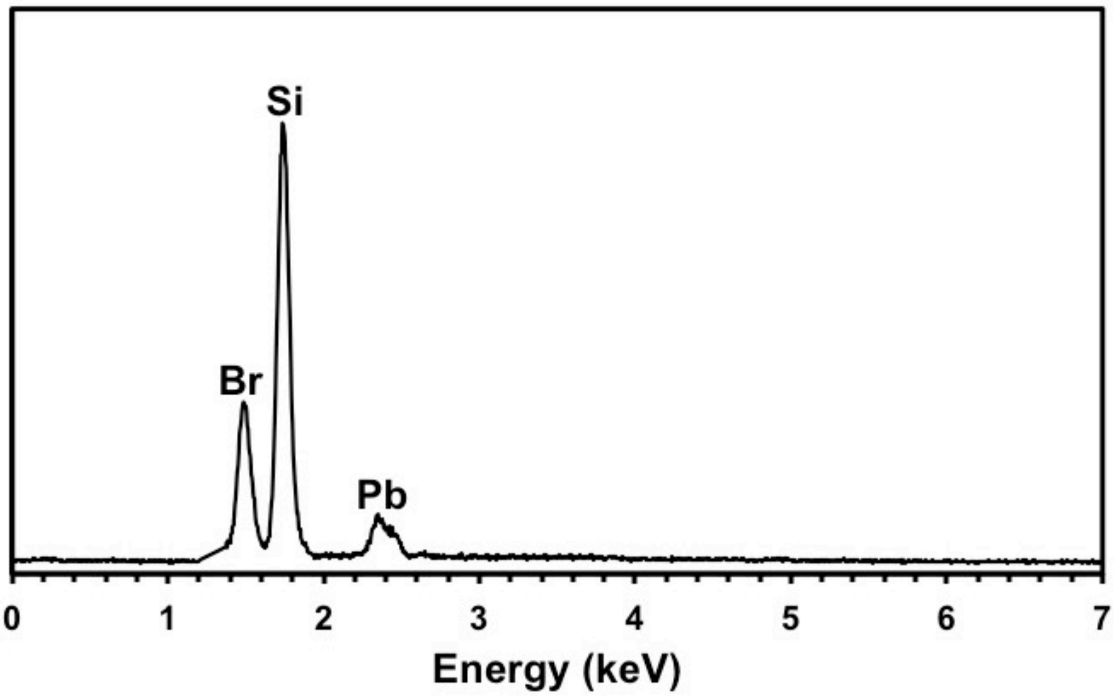

Fig. S3. A representative EDS spectrum of the ultrasmall $MAPbBr_{3.8}$ PNCs. The atomic ratio of Pb-to-Br of the original PNCs was found to be 1:3.8. This ratio is higher than the ideal 1:3 ratio reported for both the bulk $MAPbBr_3$ perovskite,[1,4] large $MAPbBr_3$ nanocrystals,[5] as well as $CsPbBr_3$ NCs.[6-8] However, it is known that ultrasmall PNCs, with subsequent larger surface area, can possess a higher Pb-to-Br ratio.[9]

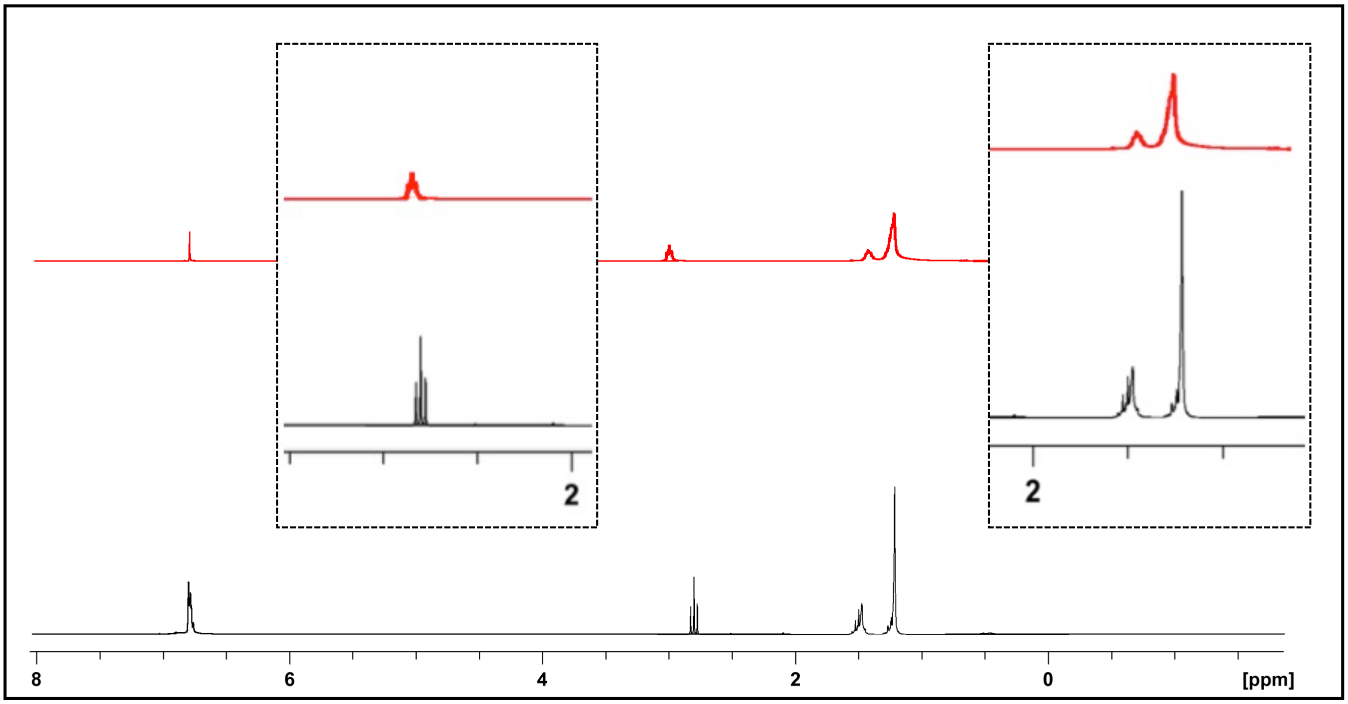

Fig. S4: NMR characterization of ultrasmall MAPbBr$_{3.8}$ PNCs. The black line is the ^{1}H NMR spectrum of the pure DADD ligand and the red line is the purified ultrasmall MAPbBr$_{3.8}$ PNCs. The characteristic amine (-N**H**$_2$) methylene (-C**H**$_2$-NH$_2$) peaks at 1.5 and 2.72 ppm, respectively, are broader in the purified PNCs than pure DADD. The peak at 1.6 ppm resembles –C**H**$_2$-CH$_2$-NH$_2$. This broadening is attributed to the transversal interproton dipolar relaxation mechanism.[10,11]

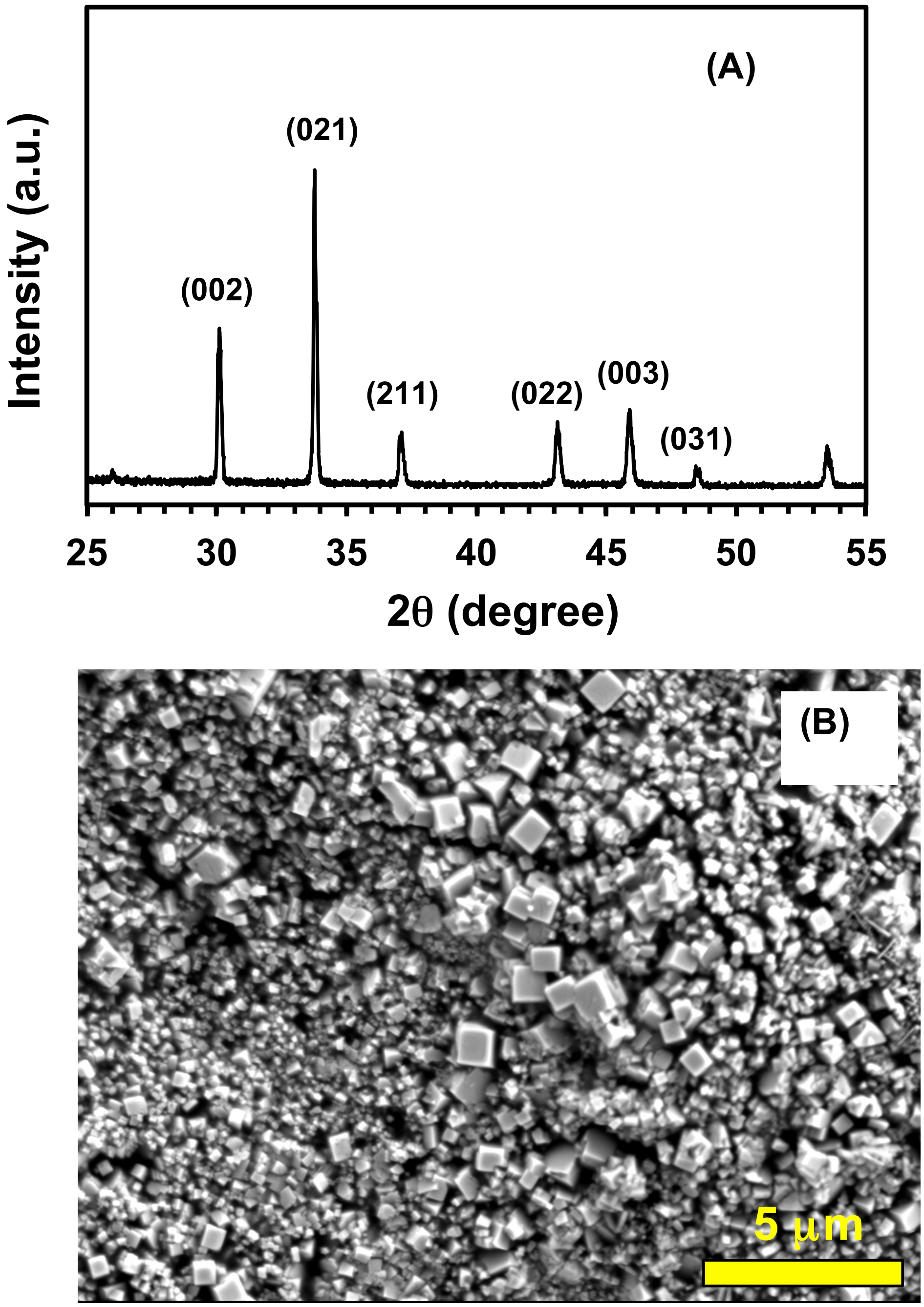

Fig. S5: Structural characterizations of Perovskite in the absence of DADD. XRD spectrum (A) and SEM (B) image of the perovskite materials prepared in the absence DADD while keeping all other experimental conditions identical as similar to white-light emitting PNCs synthesis. Bulk cubic phase, perovskite material was formed and it has been confirmed by the appearance of sharp diffraction peaks in XRD and micro-size particles in the SEM. Therefore, DADD acts as a surface passivating ligand.

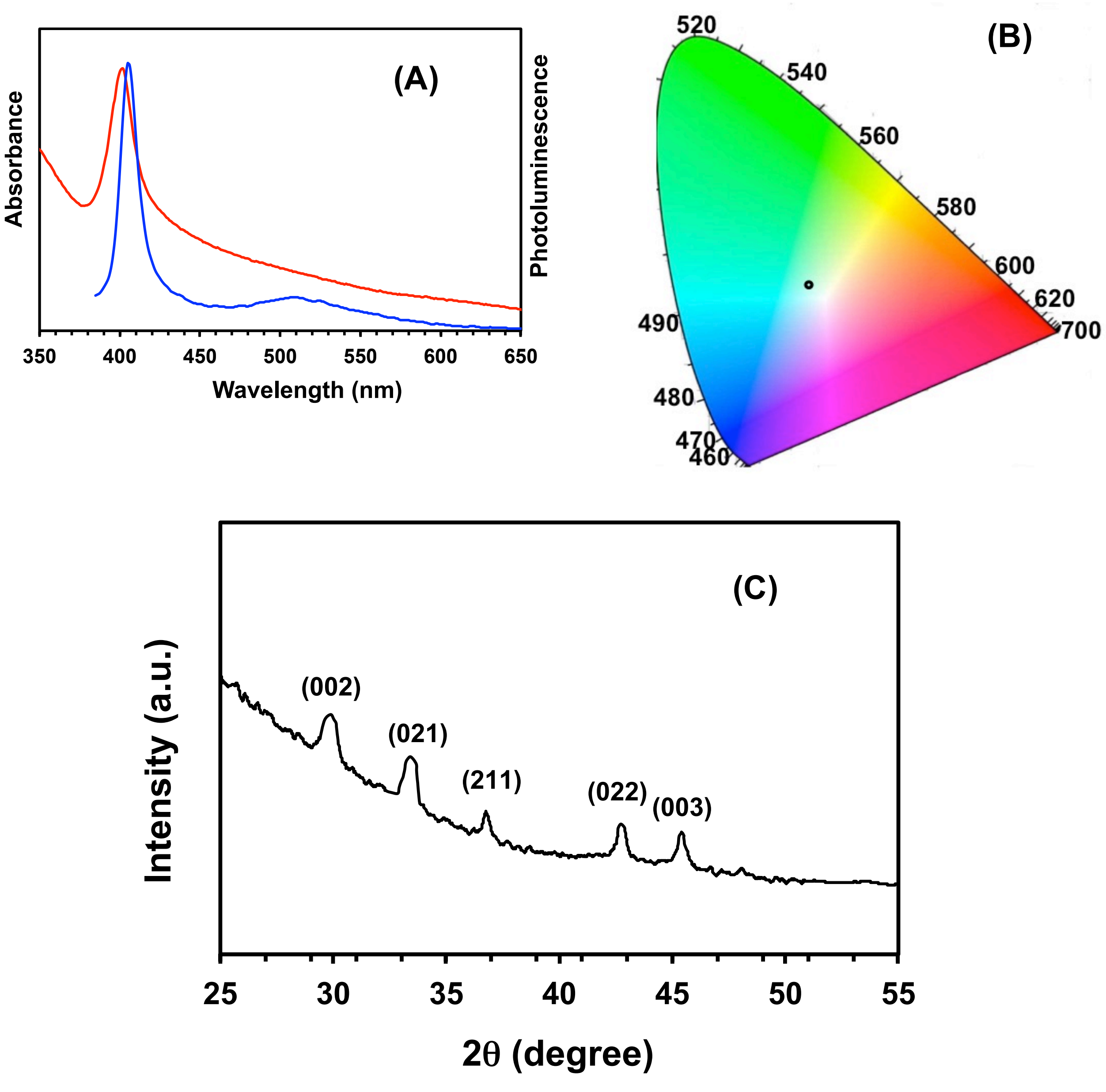

Fig. S6: Optical and structural characterizations of Perovskite materials synthesized in the absence of HA. In the absence of HA, while keeping all other reaction conditions identical, ultrasmall $MAPbBr_{3.8}$ PNCs were formed, however, due to the lesser degree of surface passivation, the emission quantum yield was reduced to ~0.6%. (A) The absorption

(402 nm) and emission (403, 512 nm) spectra of the PNCs in toluene. (B) CIE coordinates (0.338, 0.387) of the $MAPbBr_{3.8}$ PNCs. (C) The XRD pattern still matches that of cubic phase perovskite, while the broad peaks represent ultrasmall size PNCs.

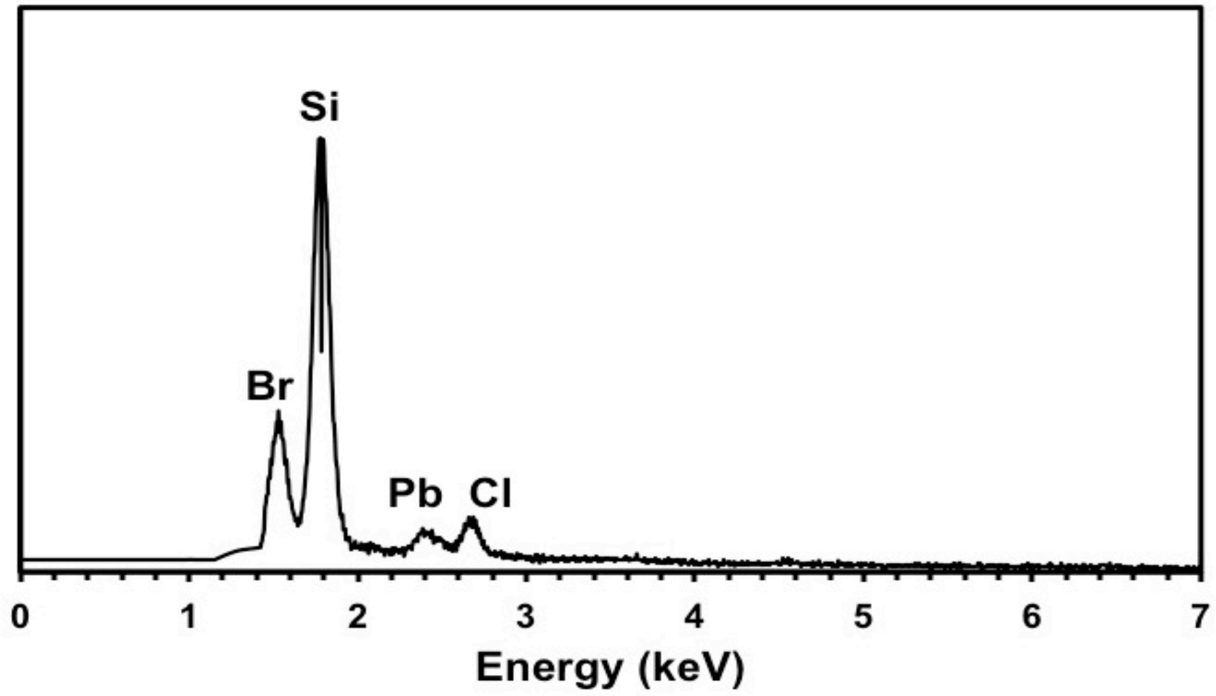

Fig. S7: Representative EDS spectrum of the ultrasmall $MAPbCl_{1.3}Br_{2.5}$ PNCs. The Pb:Cl:Br ratio suggests that chloride ions were replacing bromide ions both on the surface and in the core of the structure. This is further supported by the observed blue shift in the absorption and band edge emission peaks.

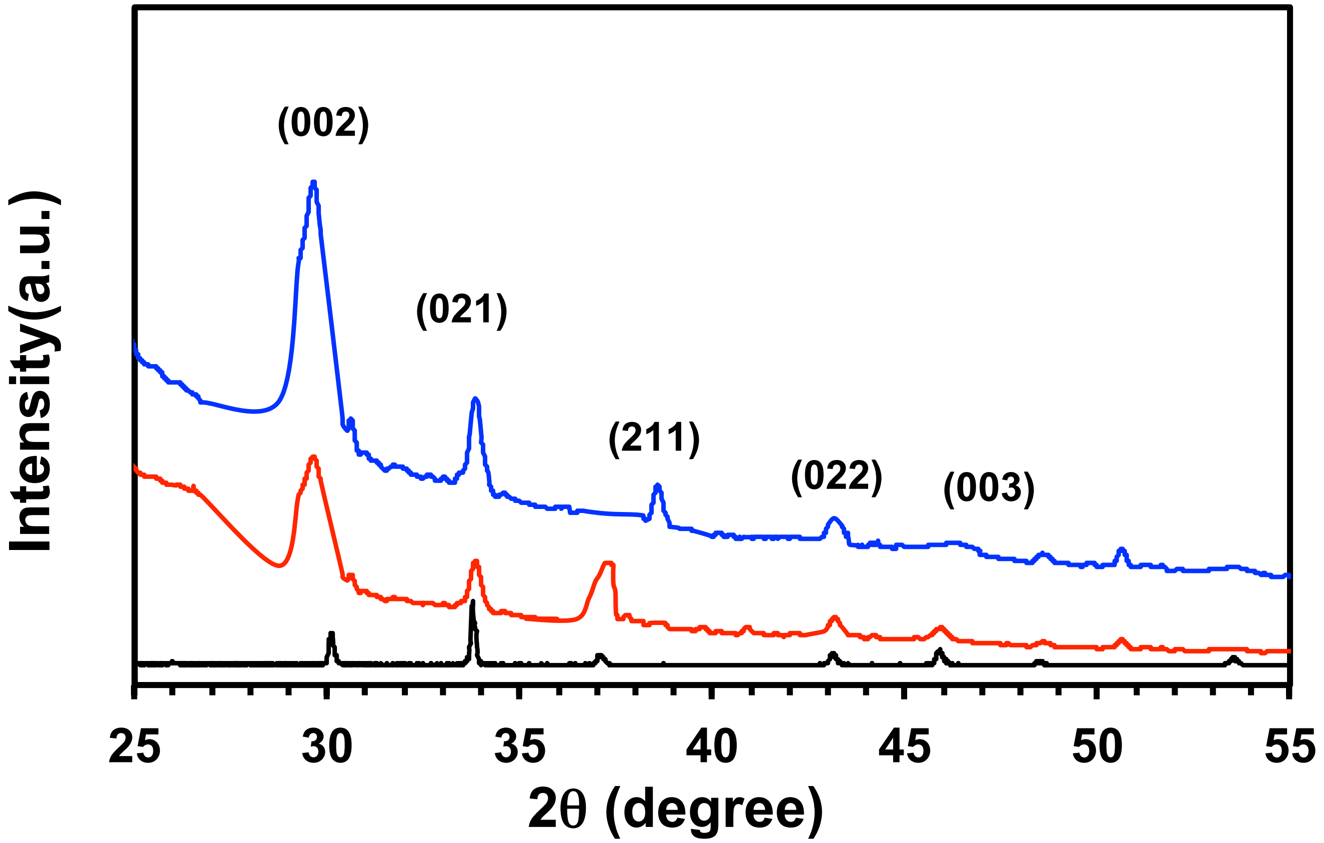

Fig. S8: XRD characterization of the different composition of perovskite materials. The XRD pattern of the $MAPbBr_{3.8}$ PNCs (red), $MAPbCl_{1.3}Br_{2.5}$ PNCs (blue), and bulk $MAPbBr_3$ perovskite. After the chloride exchange, the PNCs still maintain the cubic structure, but partial incorporation of the chloride ions results in the shift of the pattern to higher angles.[6,12]

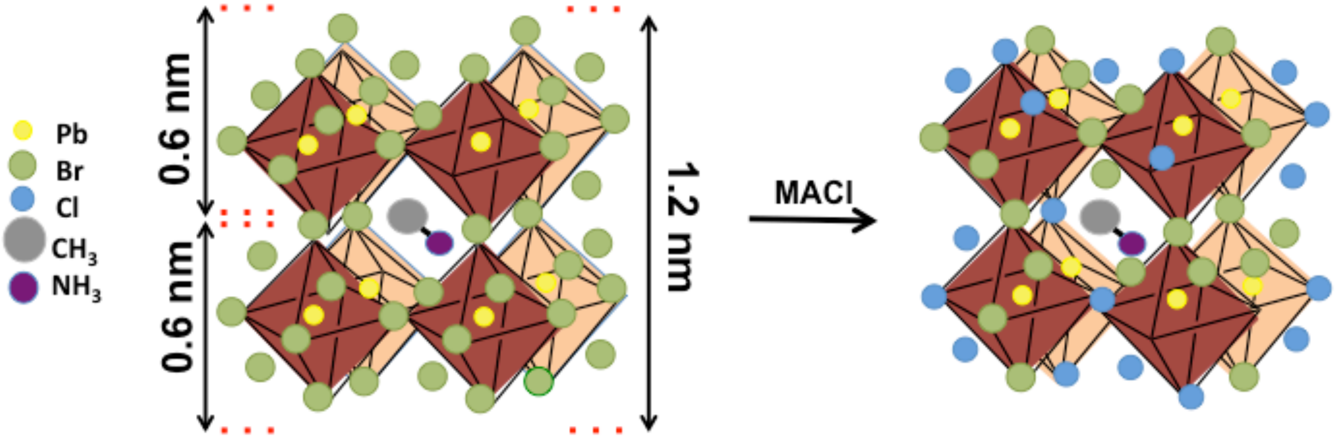

Fig. S9: Halide substitution scheme. Schematic representation of the chloride ion substitution in the $MAPbBr_{3.8}$ and resulting formation of mixed halide ($MAPbCl_{1.3}Br_{2.5}$) perovskite structure. Based on the optical data and as well as the Pb to halide ratio determined from the EDX analysis, we believe that the chloride ions are replacing all of the surface bromides and certain percentage of bromide ions in the core.

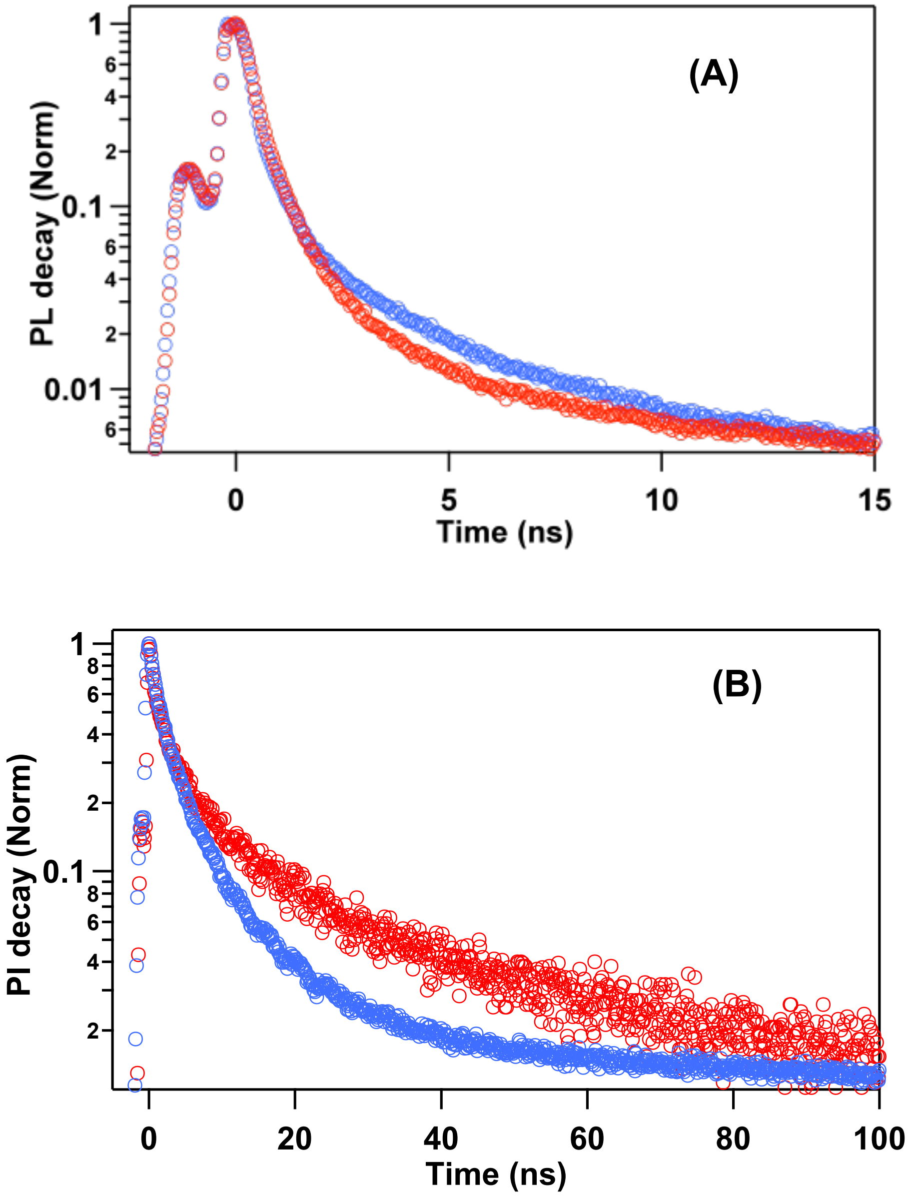

Fig. S10: Photoluminescence time decay for $MAPbBr_{3.8}$ and $MAPbCl_{1.3}Br_{2.5}$ PNCs. PL decay traces of band-edge collected at 409 nm (A) and broadband peaks collected at 515 nm (B) of $MAPbBr_{3.8}$ (blue) and $MAPbCl_{1.3}Br_{2.5}$ (red) PNCs. Stretched exponential fit of TCSPC spectra were used to determine the time constants.

References

1 Shi, D.,Adinolfi, V.,Comin, R.,Yuan, M.,Alarousu, E.,Buin, A.,Chen, Y.,Hoogland, S.,Rothenberger, A.,Katsiev, K.,Losovyj, Y.,Zhang, X.,Dowben, P. A.,Mohammed, O. F.,Sargent, E. H. and Bakr, O. M. *Science* 2015, **347**, 519-522.

2 Tan, Z.-K.,Moghaddam, R. S.,Lai, M. L.,Docampo, P.,Higler, R.,Deschler, F.,Price, M.,Sadhanala, A.,Pazos, L. M.,Credgington, D.,Hanusch, F.,Bein, T.,Snaith, H. J. and Friend, R. H. *Nat. Nano.*, 2014, **9**, 687-692.

3 van Driel, A. F.,Nikolaev, I. S.,Vergeer, P.,Lodahl, P.,Vanmaekelbergh, D. and Vos, W. L. *Phys. Rev. B*, 2007, **75**, 035329.

4 Stranks, S. D.,Eperon, G. E.,Grancini, G.,Menelaou, C.,Alcocer, M. J. P.,Leijtens, T.,Herz, L. M.,Petrozza, A. and Snaith, H. J. *Science*, 2013, **342**, 341-344.

5 Schmidt, L. C.,Pertegás, A.,González-Carrero, S.,Malinkiewicz, O.,Agouram, S.,Mínguez Espallargas, G.,Bolink, H. J.,Galian, R. E. and Pérez-Prieto, J. *J. Am. Chem. Soc.*, 2014, **136**, 850-853.

6 Akkerman, Q. A.,D’Innocenzo, V.,Accornero, S.,Scarpellini, A.,Petrozza, A.,Prato, M. and Manna, L. *J. Am. Chem. Soc.*, 2015, **137**, 10276-10281.

7 Nedelcu, G.,Protesescu, L.,Yakunin, S.,Bodnarchuk, M. I.,Grotevent, M. J. and Kovalenko, M. V. *Nano Lett.*, 2015, **15**, 5635-5640.

8 Protesescu, L.,Yakunin, S.,Bodnarchuk, M. I.,Krieg, F.,Caputo, R.,Hendon, C. H.,Yang, R. X.,Walsh, A. and Kovalenko, M. V. *Nano Lett.*, 2015, **15**, 3692-3696.

9 Zhang, F.,Zhong, H.,Chen, C.,Wu, X.-g.,Hu, X.,Huang, H.,Han, J.,Zou, B. and Dong, Y. *ACS Nano*, 2015, **9**, 4533-4542.

10 Hens, Z. and Martins, J. C. *Chem. Mater.*, 2013, **25**, 1211-1221.

11 Anderson, N. C.,Hendricks, M. P.,Choi, J. J. and Owen, J. S. *J. Am. Chem. Soc.*, 2013, **135**, 18536-18548.

12 Jang, D. M.,Park, K.,Kim, D. H.,Park, J.,Shojaei, F.,Kang, H. S.,Ahn, J.-P.,Lee, J. W. and Song, J. K. *Nano Lett.*, 2015, **15**, 5191-5199.